SETAC PRESS

Environmental Toxicology and Chemistry, Vol. 34, No. 12, pp. 2816–2823, 2015

Printed in the USA

TOXICOKINETICS AND TOXICODYNAMICS OF DIFFERENTLY COATED SILVER NANOPARTICLES AND SILVER NITRATE IN *ENCHYTRAEUS CRYPTICUS* UPON AQUEOUS EXPOSURE IN AN INERT SAND MEDIUM

EMEL TOPUZ*†‡ and CORNELIS A.M. VAN GESTEL†
†Faculty of Earth and Life Sciences, Department of Ecological Science, VU University Amsterdam, Amsterdam, The Netherlands
‡Department of Environmental Engineering, Istanbul Technical University, Maslak, Istanbul, Turkey

(Submitted 2 April 2015; Returned for Revision 2 June 2015; Accepted 14 June 2015)

Abstract: The aim of the present study was to evaluate the effect of silver nanoparticles (AgNPs) on *Enchytraeus crypticus*, applying a combined toxicokinetics and toxicodynamics approach to understand the relationship between survival and the development of internal Ag concentrations in the animals over time. Toxicity tests were conducted in medium composed of well-defined aqueous solutions added to inert quartz sand to avoid the complexity of soil conditions. Citrate-coated AgNPs (AgNP-Cit) and polyvinylpyrrolidone-coated AgNPs (AgNP-PVP) were tested and compared with silver nitrate ($AgNO_3$), which was used as a positive control for Ag ion effects. The median lethal concentration (LC50) values based on Ag concentrations in the solution phase of the test medium decreased over time and reached steady state after 7 d, with $AgNO_3$ and AgNP-PVP being more toxic than AgNP-Cit. Slow dissolution may explain the low uptake kinetics and lower toxicity of AgNP-Cit compared with the other 2 Ag forms. The LC50 values based on internal Ag concentrations in the animals were almost stable over time, highlighting the importance of integrating toxicokinetics and toxicodynamics and relating survival with internal Ag concentrations. Neither survival-based elimination rates nor internal LC50s in the organisms showed any significant evidence of nano-specific effects for both AgNPs, although they suggested some uptake of particulate Ag for AgNP-Cit. The authors conclude that the toxicity of both types of AgNP probably is mainly attributable to the release of Ag ions. *Environ Toxicol Chem* 2015;34:2816–2823. © 2015 SETAC

Keywords: Uptake kinetics Bioavailability Citrate Polyvinylpyrrolidone

INTRODUCTION

Silver nanoparticles (AgNPs) have been used in an increasing number of consumer products [1], and ecosystems might be exposed to AgNPs as a result of their possible release from these products into the environment [2]. The release of AgNPs from textiles has already been proved by a few recent studies [3–5]. It is likely that they will end up in wastewater treatment systems and ultimately in receiving environmental media such as surface waters and soils [6]. Several studies are dealing with the possible consequences of the presence of AgNPs in aquatic environments. These studies conclude that AgNPs may cause substantial harm at very low concentration levels (micrograms per liter) to various species of aquatic organisms such as the algae *Pseudokirchneriella subcapitata* and *Chlamydomonas reinhardtii* [7,8], the water flea *Daphnia magna* [8,9], and the fish *Danio rerio* [8,10].

Soil organisms are also likely exposed to AgNPs, which may partition to sediments or soil media because of agglomeration over time, depending on the water chemistry [11]. In addition, AgNPs that enter wastewater treatment plants mostly partition to the sewage sludge fraction during treatment [12], and soil organisms might be exposed to AgNPs through the land application of sewage sludge [13]. Therefore, it also is essential to investigate the possible interactions of AgNPs for a diverse range of soil organisms. However, the fate of AgNPs in soil is even more complicated than that in water because of their interaction with both the soil solution and the soil stationary phase [14]. The complexity of the behavior of AgNPs in aquatic media is usually the result of their agglomeration/aggregation and/or dissolution rates, which may vary depending on the presence of various dissolved inorganic/organic compounds and/or colloids [15]. Similar processes also play an important role in soil [16]. Thus, it would be better to figure out the exposure of soil organisms to AgNPs at the soil–solution interface and its consequent effects. This relation may be more accurately investigated by integrating toxicokinetics (uptake and elimination of the compound over time) and toxicodynamics (effects on the organism over time) approaches [17].

In addition to the environmental factors, the properties of AgNPs, which are mainly dependent on their capping agents, are determining variations in their environmental fate and effects [18]. Therefore, such studies may also provide substantial knowledge on the difference in toxicity of AgNPs with different capping agents.

Hence, the aim of the present study was to investigate the toxicokinetics and toxicodynamics of AgNPs with different coatings in a model soil organism and understand the relationship between survival and the development of internal Ag concentrations in the animals over time. Silver nanoparticles coated with citrate (AgNP-Cit) or polyvinylpyrrolidone (AgNP-PVP), which are among the most widely used in products, were tested and compared, and ionic Ag ($AgNO_3$) exposures were included for comparison. *Enchytraeus crypticus* were chosen as the test species, because they are ecologically relevant soil organisms that play a crucial role in decomposition and bioturbation in soils [19]. Enchytraeids are commonly used for toxicity testing because of their sensitivity to a wide range of stressors [20]. To avoid disturbance by complex environmental

All Supplemental Data may be found in the online version of this article.
*Address correspondence to topuze@itu.edu.tr
Published online 19 June 2015 in Wiley Online Library (wileyonlinelibrary.com).
DOI: 10.1002/etc.3123

conditions usually affecting the fate of nanoparticles and released metal ions in soil, the uptake, elimination, and toxicity of ionic Ag and AgNPs were determined in a medium composed of well-defined aqueous solutions added to inert quartz sand. This medium was shown to provide a convenient living medium for the test organisms [17].

MATERIALS AND METHODS

Test organisms

Enchytraeus crypticus (Enchytraeidae; Oligochaeta; Annelida) has been cultured for more than 10 yr in the laboratory of the Department of Ecological Science, VU University, Amsterdam, The Netherlands. Details about culturing the test organisms have been explained in Castro-Ferreira et al. [19]. Briefly, *E. crypticus* were cultured in agar media prepared with soil extract and kept in the dark in a climate room at constant temperature (16 °C) and relative humidity (75%). The culture was fed twice a week with a mixture of oatmeal, dried yeast, egg yolk powder, and fish oil. For the experiments, adult *E. crypticus* with white spots in the clitellum region were selected.

Test compounds and test medium

In the present study, AgNPs, AgNP-PVP, AgNP-Cit, and ionic silver in the form of $AgNO_3$ were tested; $AgNO_3$ also served as a positive control to distinguish possible effects originating from nanoparticles from those of the released Ag^+ ions. Both AgNP-Cit and AgNP-PVP were purchased from NanoSys GmBH and obtained as suspensions in water at concentrations of 1 g/L and 10 g/L AgNPs, respectively. Ionic silver (Sigma-Aldrich; >99%) was dissolved in deionized water. The nominal size of AgNP-Cit and AgNP-PVP provided by the manufacturer was approximately 25 nm; detailed characterization of both AgNPs has been reported in Topuz et al. [11].

The experiments were conducted in quartz sand, which was pretreated to obtain an inert matrix free of residuals such as organic carbon. Pretreatment of quartz sand and its characteristics have been explained in detail by He and van Gestel [17]. In brief, after combustion at 600 °C for 2 h, the quartz sand was rinsed with 0.7 M HNO_3 (Sigma-Aldrich; 65%), tap water, and deionized water and finally air-dried.

The test medium was prepared by dissolving $Ca(NO_3)_2$, $MgSO_4$ $7H_2O$, $NaNO_3$, and KNO_3 (Sigma-Aldrich; >99%) in deionized water. The test medium was diluted by spiking with $AgNO_3$ or AgNP stock solution to prepare the test solutions with the desired Ag test concentrations and ionic concentrations of 0.2 mM Ca^{2+}, 0.05 mM Mg^{2+}, 2.0 mM Na^+, and 0.078 mM K^+. Because of its known influence on the speciation of silver, the use of chloride was avoided in the test medium. The pH of the test solutions was adjusted to approximately 6.0 using 0.75 g/L 3-(*N*-morpholino]) propane sulfonic acid (AppliChem; >99%), 0.75 mg/L 2-(*N*-morpholino) ethane sulfonic acid (Sigma-Aldrich; >99%) or 1 mM NaOH (Sigma-Aldrich; >99%), if needed.

Toxicity tests

Toxicity tests were designed according to the results of preliminary experiments in which *E. crypticus* were exposed to 10 mg/L of Ag and AgNPs for 7 d in triplicate. All animals died in the presence of $AgNO_3$, whereas survival rates were $90 \pm 0\%$ and $43 \pm 40\%$ for AgNP-Cit and AgNP-PVP, respectively. Based on these results, nominal external test concentrations selected were 1.5625 mg Ag/L, 3.125 mg Ag/L, 6.25 mg Ag/L, 12.5 mg Ag/L, 25 mg Ag/L, and 50 mg Ag/L for AgNP-Cit and AgNP-PVP to be able to obtain a full dose–response curve and to compare the toxicity of the AgNPs. For $AgNO_3$, concentrations tested were 0.5 mg Ag/L, 1 mg Ag/L, 2 mg Ag/L, 4 mg Ag/L, 8 mg Ag/L, and 16 mg Ag/L. Controls without Ag were also included. Five different time points (2 d, 3 d, 5 d, 7 d, and 10 d) were selected to determine the effect of exposure time on Ag bioaccumulation and on survival as the toxicity end point. Three replicates were prepared for each test concentration and time point.

After placing 20 g of pretreated quartz sand in glass jars (100 mL), 6 mL of test solution were added and the sand–solution mixture was conditioned overnight. The experiments were started by the introduction of 10 adult *E. crypticus* into each jar. The jars were covered with perforated aluminum foil to limit water loss and kept in a climate room at 20 ± 1 °C under a 12:12-h light:dark cycle. Water evaporation was checked twice per week, and deionized water was added if necessary. At each time point, *E. crypticus* was collected from 3 jars per treatment after the addition of 5 mL of deionized water, counted to determine survival, and frozen at –18 °C for Ag analysis. Test solutions were filtrated through 0.45-μm membrane filters (Pall), which had been conditioned with 0.1 M $Cu(NO_3)_2$ (Alfa Aesar; purity >98%) to prevent Ag loss by sorption to the filters [21]. Filtered samples were stored at +4 °C for Ag analysis after adding 0.625 mL of concentrated HCl (Sigma-Aldrich; 37%) and 0.275 mL H_2O_2 (Sigma-Aldrich; 35%). The glass jars with sand matrix were opened and stored under the fume hood to evaporate until dryness before extraction for Ag analysis.

Ag analysis

Enchytraeus crypticus, filtered test solutions, and sand matrix were analyzed for total Ag at the end of the toxicity tests. *Enchytraeus crypticus* were freeze-dried overnight, weighed using an analytical balance, and transferred into thoroughly cleaned Pyrex glass tubes. After placing the tubes on a hot plate, 300 μL of a mixture of concentrated HNO_3 (Mallbaker Ultrex Ultra Pure; 65%) and $HClO_4$ (Mallbaker Ultrex Ultra Pure; 70%) (7:1) was added. The animals were digested in different heating steps at 85 °C, 120 °C, and 165 °C for 30 min, 30 min, and 45 min, respectively, after which the digestion mixture was completely evaporated at 180 °C. Residues were taken up in 1 M HCl for Ag measurements.

Test solutions and sand were digested following the method described in Ribeiro et al. [8] for total Ag measurements. Filtered test solutions were shaken at 100 rpm for 24 h and evaporated to around 1 mL in a water bath at 50 °C. Then, 3 mL of concentrated HCl (Sigma-Aldrich; 35%) and 1 mL of concentrated HNO_3 (Sigma-Aldrich; 65%) were added to digest the samples for 1 h in the same water bath. Digested samples were made up to 50 mL with 1 M HCl in polyprolydine Falcon tubes for the measurements. Completely dried sand samples were extracted by adding 10 mL of deionized water, 0.625 mL concentrated HCl, and 0.275 mL H_2O_2 and shaking the mixture at 100 rpm for 24 h. Supernatants were filtered over 0.45-μm membrane filters conditioned with 0.1 M $Cu(NO_3)_2$. Analyses were conducted by graphite furnace atomic absorption spectrophotometry (Perkin Elmer 5100ZL and Analytic-Jena contrAA 700).

Kinetic calculations

Internal Ag concentrations in *E. crypticus* (C_0; mg/kg dry body wt) as a function of time (t) were calculated with a

1-compartment model, assuming that exposure concentration (C_w; mg Ag/L) was constant over time (Equation 1)

$$C_0(t) = \frac{K_w \times C_w}{K_{e1}} \times (1 - e^{-K_{e1} \times t}) \quad (1)$$

where K_w is the uptake rate constant (L/kg dry body wt/d) and K_{e1} is the elimination rate constant (1/d).

To link Ag concentrations in *E. crypticus* (C_0; in mg Ag/kg dry body wt) after 7 d with exposure concentrations in the water fraction of the test medium (C_w; mg Ag/L), a Langmuir equation was applied

$$C_0 = \frac{K_L \times C_{max} \times C_w}{1 + K_L \times C_w} \quad (2)$$

where C_{max} (mg/kg dry body wt) is the maximum internal Ag concentration that can be accumulated by the enchytraeids and K_L is the adsorption coefficient (L/kg dry body wt), which may indicate affinity of the different Ag forms for uptake by the test animals.

Lethal concentrations killing 50% of the test organisms (LC50) at the different points in time were calculated with the trimmed Spearman-Karber method [22]. The LC50 value (mg Ag/L) can also be expressed as a function of time as

$$LC50(t) = \frac{LC50\infty}{1 - e^{-K_{e2} \times t}} \quad (3)$$

where LC50∞ is the ultimate LC50 (mg Ag/L) and K_{e2} is the survival-based elimination rate constant (1/d). Lethal body concentration (LBC; mg/kg dry body wt) was related to LC50∞ (mg Ag/L) using K_w (L/kg dry body wt/d) and K_{e1} (1/d)

$$LBC = LC50\infty \times \frac{K_w}{K_{e1}} \quad (4)$$

The relationship between survival (S; %) and time (t; days) was determined with a logistic survival model

$$S(t) = \frac{e^{-\mu \times t}}{1 + \left(\frac{C_w}{LC50(t)}\right)^b} \quad (5)$$

where C_w (mg Ag/L) is the exposure concentration, μ is the natural mortality rate (1/d), LC50(t) is LC50 determined at time t, and b is the slope factor.

Logistic dose–response equations were also used for analyzing the relationship between survival (S; %) and internal Ag concentrations in the organisms (C_0; mg/kg dry body wt)

$$S = \frac{S_0}{1 + \left(\frac{C_0}{LC50inter}\right)^b} \quad (6)$$

where S_0 is the control survival (%), LC50inter is the median lethal concentration based on internal Ag concentrations (mg/kg dry body wt), and b is the slope parameter.

Statistical Analysis

The IBM SPSS Statistics 21 package was used for all kinetic calculations and statistical analyses. Nonlinear regression analyses were used to fit corresponding equations to the data to obtain overall Ag uptake (K_w) and elimination (K_{e1}) rate constants, natural mortality rate (μ) and survival-based elimination (K_{e2}) rate constants, and LC50∞, and LC50inter. Estimated parameters for $AgNO_3$, AgNP-Cit, and AgNP-PVP were compared using likelihood ratio tests.

RESULTS

Measured Ag concentrations in the spike solutions generally were in agreement with nominal ones, with recoveries higher than 80% (Supplemental Data, Table S1). Concentrations of Ag in the sand (Supplemental Data, Table S2) and solution (Supplemental Data, Table S3) fractions of the test medium, measured after 2 d and 7 d, did not differ much, which demonstrates constant exposure conditions during the time period used in the present study. Most of the Ag was partitioned to the sand (see Supplemental Data, Tables S2 and S3). Recoveries of the spiked Ag, calculated from a mass balance of sand and solution phase concentrations, mostly were acceptable at 80% to 120% (Supplemental Data, Table S4). Toxicity, toxicokinetics, and toxicodynamics of the different Ag forms are related to the average Ag concentrations measured in the solution phase of the test medium reported in Supplemental Data, Table S3.

Survival decreased with increasing time and exposure concentration (Figure 1). At the highest 3 concentrations of $AgNO_3$ (0.215–0.595 mg Ag/L) and AgNP-PVP (0.348–1.08 mg Ag/L), survival reached steady state within 7 d of exposure, whereas steady state was reached within 10 d of exposure for the lower concentrations. For AgNP-Cit, steady state was reached after 7 d at all test concentrations.

Total Ag concentrations taken up by *E. crypticus* are shown in Supplemental Data, Tables S5 to S7, and plotted against time in Figure 2. The uptake of silver from $AgNO_3$ and both AgNPs was affected by time and exposure concentration. Body concentrations approached steady state after 7 d of exposure. No data were obtained for the highest 2 concentrations of $AgNO_3$ (0.293 mg Ag/L and 0.595 mg Ag/L) and AgNP-PVP (0.48 mg Ag/L and 1.08 mg Ag/L), where all animals died. The highest total Ag concentrations in *E. crypticus* measured were 28.1 mg Ag/kg, 125 mg Ag/kg, and 77.5 mg Ag/kg for $AgNO_3$ (at 0.215 mg Ag/L), AgNP-Cit (at 9.57 mg Ag/L), and AgNP-PVP (at 0.348 mg Ag/L) after 7 d, 10 d, and 5 d of exposure, respectively.

When all data points for all concentrations and sampling times were fitted to Equation 1, the overall K_w (uptake) and K_{e1} (elimination) rate constants for $AgNO_3$, AgNP-Cit, and AgNP-PVP were 49.5 L/kg dry body weight/d, 3.62 L/kg dry body weight/d, and 45.8 L/kg dry body weight/d and 0.259 1/d, 0.231 1/d, and 0.071 1/d, respectively (Table 1). The R^2 values for the model fit (Figure 2) ranged from 0.318 to 0.415 for $AgNO_3$ and AgNP-Cit to 0.876 for AgNP-PVP. The K_W and K_{e1} values for AgNP-Cit and AgNP-PVP were significantly different ($\chi^2 = 10.8$ and 17.8, respectively; $p < 0.05$). The K_w value increased with increasing exposure concentration up to 0.037 mg Ag/L, 0.212 mg Ag/L, and 0.072 mg Ag/L for $AgNO_3$, AgNP-Cit, and AgNP-PVP, respectively, and then decreased again with increasing concentration (see Supplemental Data, Tables S5–S7). Bioconcentration factors (BCFs) calculated from the overall K_w and K_{e1} values were 190, 16, and 646, respectively (Table 1); but the BCFs for the AgNPs especially are flattered by deviating values at the highest exposure levels, where uptake probably was hampered by high toxicity (Figure 1; Supplemental Data, Tables S5–S7). Omitting the higher concentrations led to average BCFs of approximately

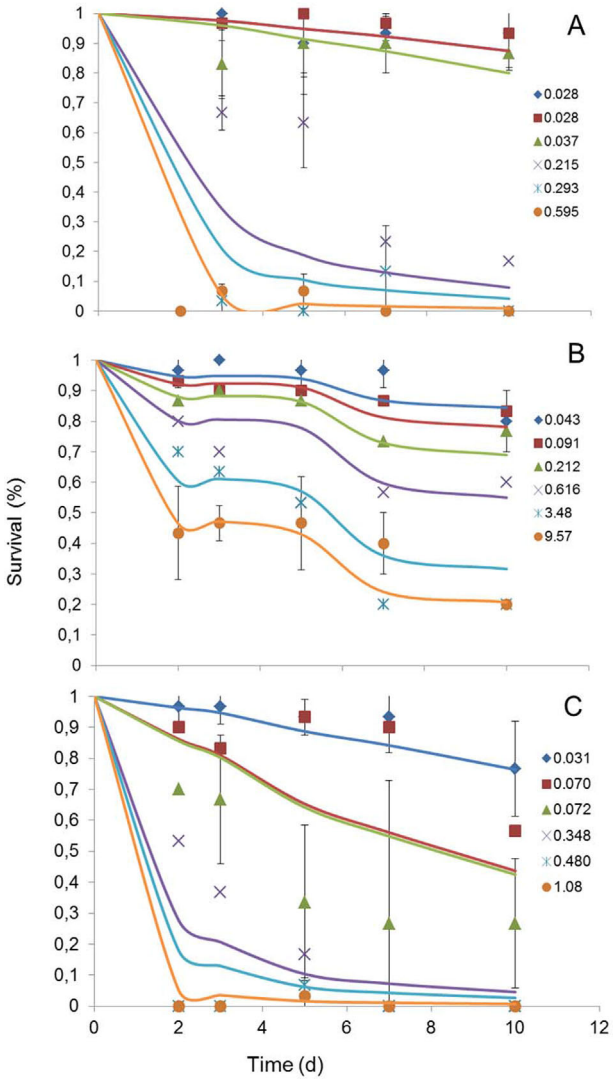

Figure 1. Development with time of the survival of *Enchytraeus crypticus* exposed to (**A**) $AgNO_3$, (**B**) citrate-coated Ag nanoparticles, and (**C**) polyvinylpyrrolidone-coated Ag nanoparticles in a sand-solution medium. Exposure concentrations are measured concentrations in the solution phase of the sand-solution medium (in mg Ag/L; obtained after 0.45-μm filtration). Data points show survival at different sampling times, and solid lines represent the fit of a logistic dose–response model (Equation 5) to the data. Error bars represent the standard deviations of the survival in triplicate experiments.

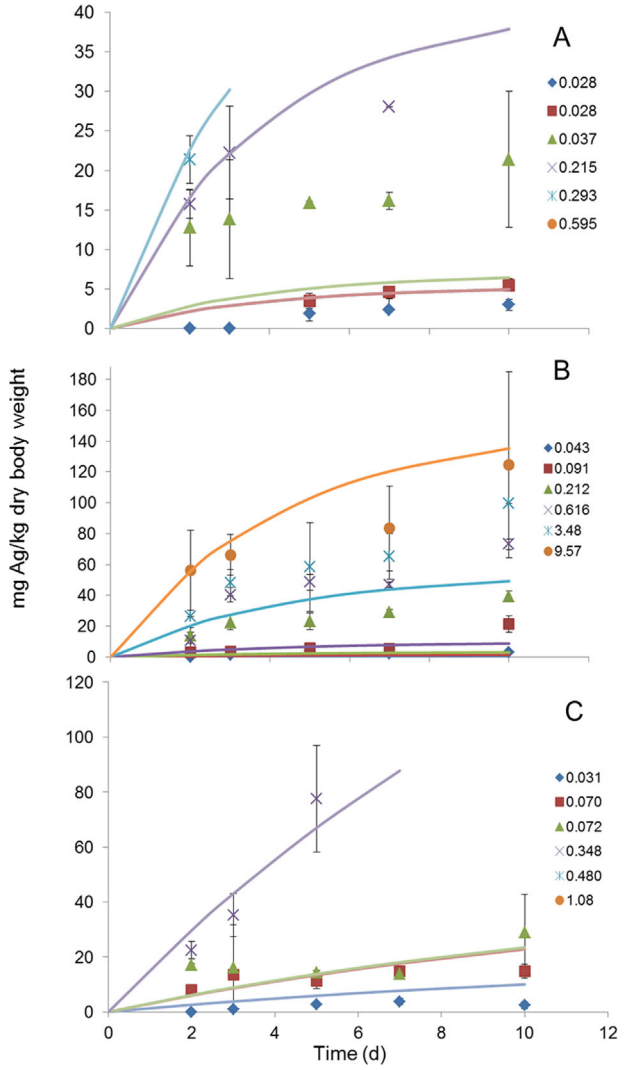

Figure 2. Development with time of internal total Ag concentrations in *Enchytraeus crypticus* exposed to (**A**) $AgNO_3$, (**B**) citrate-coated Ag nanoparticles, and (**C**) polyvinylpyrrolidone-coated Ag nanoparticles in a sand-solution medium. Data points show the measured total Ag concentrations in *E. crypticus* at each sampling time, and solid lines represent the fit of the 1-compartment model (Equation 1) to the data for the different measured exposure concentrations in the solution phase of the sand-solution medium (in mg Ag/L; obtained after 0.45-μm filtration). Error bars represent the standard deviations of the concentrations measured in triplicate samples.

150 L/kg and 205 L/kg for AgNP-Cit and AgNP-PVP, respectively.

When all Ag uptake data for all concentrations after 7 d of exposure were fitted to Equation 2, Langmuir adsorption coefficients (K_L) and maximum internal Ag concentrations (C_{max}) were estimated at 1.53 L/kg dry body weight, 1.80 L/kg dry body weight, and 7.47 L/kg dry body weight and 58.7 mg Ag/kg dry body weight, 44.4 mg Ag/kg dry body weight, and 84.4 mg Ag/kg dry body weight for $AgNO_3$, AgNP-Cit, and AgNP-PVP, respectively (Table 1; Supplemental Data, Figure S1). Neither the K_L and nor the C_{max} values of $AgNO_3$ and the AgNPs were significantly different ($\chi^2 < 3.84$, not significant).

After 10 d of exposure, LC50 values for the effect of $AgNO_3$, AgNP-Cit, and AgNP-PVP on enchytraeid survival based on Ag concentrations in the spike solutions were 1.53 mg Ag/L, 15.9 mg Ag/L, and 3.37 mg Ag/L, respectively. The LC50 values based on measured concentrations in the solution phase of the test medium for AgNP-Cit and AgNP-PVP decreased from 7.43 mg Ag/L to 0.88 mg Ag/L and from 0.2 mg Ag/L to 0.06 mg Ag/L, respectively, in 10 d. For $AgNO_3$, LC50 decreased from 0.15 mg Ag/L to 0.07 mg Ag/L (Figure 3). The R^2 values for the fit of LC50 versus time using Equation 3 ranged from 0.709 for AgNP-Cit to 0.982 for AgNP-PVP (Table 1). Silver nitrate and AgNP-PVP had the lowest ultimate LC50∞ (0.047 mg Ag/L and 0.081 mg Ag/L, respectively); the LC50∞ for AgNP-Cit (0.322 mg Ag/L) was higher (Table 1). Especially because of the large error for LC50∞ for AgNP-Cit, there was no significant difference between LC50∞ values. Survival-based elimination rates (K_{e2}) determined with Equation 3 were 0.324 1/d, 0.018 1/d, and 0.129 1/d for $AgNO_3$, AgNP-Cit, and AgNP-PVP, respectively (Table 1). The K_{e2} value was significantly different for $AgNO_3$ and AgNP-Cit ($\chi^2 = 18.0$, $p < 0.05$). Lethal body concentrations, which were related to LC50∞ with Equation 4, were 15.5 mg Ag/kg dry

Table 1. Estimated toxicokinetic and toxicodynamic parameters (±standard error) for the uptake and toxicity of Ag in *Enchytraeus crypticus* upon exposure to $AgNO_3$, AgNP-Cit, and AgNP-PVP in quartz sand-solution medium

Parameter	Symbol	Unit	$AgNO_3$		AgNP-Cit		AgNP-PVP		Equation
			Value	R^2	Value	R^2	Value	R^2	
Uptake rate	K_w	L/kg dry body weight/d	49.5 ± 18.5	0.318	3.62 ± 1.46	0.415	45.8 ± 8.01	0.876	1
Elimination rate	K_{e1}	1/d	0.259 ± 0.190		0.231 ± 0.151	0	0.071 ± 0.069		1
Bioconcentration factor	BCF	L/kg	190		16		645		K_w/K_{e1}
Mortality rate	μ	1/d	0.000 ± 0.006	0.939	0.000 ± 0.005	0.895	0.000 ± 0.011	0.800	5
Slope	*b*	—	2.07 ± 0.302	0.971	0.552 ± 0.064		1.73 ± 0.000		5
10-d LC50		mg/L	0.07		0.88		0.06		—
Ultimate LC50	LC50∞	mg Ag/L	0.081 ± 0.019	0.736	0.322 ± 3.54	0.709	0.047 ± 0.011	0.982	3
Survival-based elimination rate	K_{e2}	1/d	0.324 ± 0.137		0.018 ± 0.209		0.129 ± 0.038		3
Internal lethal concentration	LC50inter	mg Ag/kg dry body weight	21.8 ± 1.84	0.567	57.6 ± 4.04	0.851	21.8 ± 3.85	0.611	6
Slope	*b*	—	4.21 ± 1.64		1.51 ± 0.215	0.851	1.45 ± 0.497		6
Lethal body concentration	LBC	mg Ag/kg dry body weight	15.5		5.06		30.4		4
Adsorption coefficient	K_L	L/kg dry body weight	1.53 ± 1.17	0.943	1.80 ± 0.692	0.863	7.47 ± 5.01	0.735	2
Maximum Ag concentration in *E. crypticus*	C_{max}	mg Ag/kg dry body weight	58.7 ± 28.1		84.4 ± 7.88	0.863	50.8 ± 15.8		2

[a]All parameters were estimated by fitting different equations to the data, using measured Ag concentrations in the solution phase of the test medium (see Supplemental Data, Table S3). See Figures 1–4 for the corresponding curves showing toxicity–time relationships, uptake curves, and relating toxicity to accumulated Ag concentrations in the test organisms. See the text for the equations used.
AgNP-Cit = citrate-coated Ag nanoparticle; AgNP-PVP = polyvinylpyrrolidone-coated Ag nanoparticle; LC50 = 50% lethal concentration.

Figure 3. Median lethal concentration (LC50) for the effect of (**A**) $AgNO_3$, (**B**) citrate-coated Ag nanoparticles, and (**C**) polyvinylpyrrolidone-coated Ag nanoparticles on the survival of *Enchytraeus crypticus* upon exposure in a sand-solution medium for different periods of time. Data points show values calculated with the trimmed Spearman-Karber model [22] expressed on the basis of average measured concentrations in the solution phase of the test medium (see Supplemental Data, Table S3), and solid lines represent the fit of Equation 3 to the data.

body weight, 48.3 mg Ag/kg dry body weight, and 9.6 mg Ag/kg dry body weight, respectively, when using the overall BCF estimated from uptake kinetics for $AgNO_3$ and the average BCFs over the lower exposure concentrations for the AgNPs (Table 1).

Natural mortality rate, μ (calculated with Equation 5), was 0 d^{-1} for all 3 Ag forms (Table 1). Although the survival-time data fitted very well to the logistic survival model, with $R^2 > 0.8$ for all 3 Ag forms (Figure 1), natural mortality rate constants showed quite high variability (Table 1).

The LC50inter values calculated with Equation 6 were almost equal for $AgNO_3$ and AgNP-PVP, at 21.8 mg Ag/kg dry body weight, and much higher for AgNP-Cit (57.7 mg Ag/kg dry body weight; Table 1). The latter value was significantly different from those for $AgNO_3$ and AgNP-PVP according to the likelihood ratio test ($\chi^2 = 12.7$ and $\chi^2 = 12.6$, respectively; $p < 0.05$). The R^2 values for the fit of all data to Equation 6 (Figure 4) ranged from 0.57 for $AgNO_3$ to 0.85 for AgNP-Cit. When the data for each time point were fitted to Equation 6 individually, LC50inter for each time point did not differ significantly for all Ag compounds.

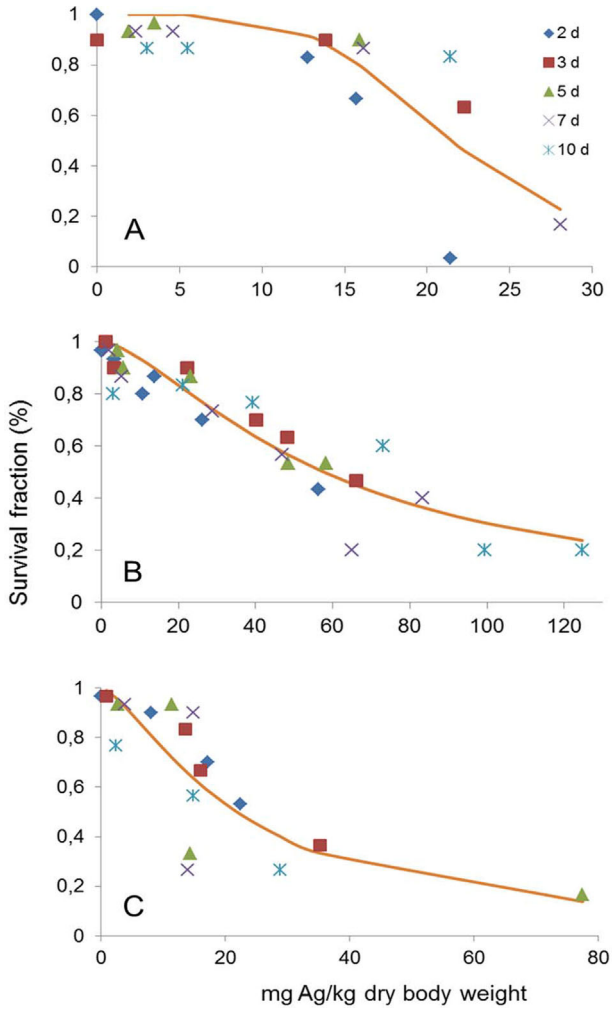

Figure 4. The relation between the survival of *Enchytraeus crypticus* and total-body Ag concentrations in animals after different times of exposure to (**A**) $AgNO_3$, (**B**) citrate-coated Ag nanoparticles, and (**C**) polyvinylpyrrolidone-coated Ag nanoparticles in a sand-solution medium. Data points stand for the measured total Ag concentrations in surviving *E. crypticus* at different sampling times, and solid lines represent the fit of a logistic dose–response equation (Equation 6) to the data.

DISCUSSION

The present study showed that, when related to the dissolved Ag fraction in the 0.45-μm filtered solution phase of the test medium, AgNP-PVP and $AgNO_3$ were about 10 times more toxic to *E. crypticus* than AgNP-Cit. Uptake and toxicity of all 3 Ag forms reached steady state after 7 d to 10 d. Internal LC50s did not change much with time and were about twice as high for AgNP-Cit as the values for the other 2 Ag forms.

Ag concentrations in the test medium

Our results also showed that only a fraction of the total dose was present in the solution phase of the test medium in the case of $AgNO_3$ (Supplemental Data, Table S3). This indicates that, although we expected the sand medium to be inert, it still did bind a considerable amount of ionic Ag. We found similar concentrations of Ag in the solution phase of our test medium for $AgNO_3$ and AgNP-PVP. Considering the expected higher sorption of AgNPs, the Ag concentrations for AgNP-PVP are in agreement with its dissolution in aqueous media reported by Odzak et al. [23] in which the same AgNP-PVPs were used. Therefore, it seems that the concentration of ionic Ag in the solution phase of the test medium was similar for $AgNO_3$ and AgNP-PVP. This seems, however, not to be the case for AgNP-Cit, where at the same total concentrations as for AgNP-PVP much higher Ag concentrations were measured in the solution phase of the test medium. This could, on the one hand, be the result of the higher affinity of the more lipophilic AgNP-PVP for binding to the sand and, on the other hand, suggest a higher release of Ag^+ ions or that part of the AgNP-Cit did pass the 0.45-μm filter.

Toxicity of different Ag forms to E. crypticus

Most studies in the literature report higher toxicity of $AgNO_3$ to soil organisms compared with AgNPs. The 50% effective concentration for the effects of AgNPs on the reproduction of *Enchytraeus albidus*, *Eisenia andrei*, and *Folsomia candida* was significantly higher than that for $AgNO_3$ [24–26]. Likewise, the survival of *Eisenia fetida* [27] and *E. andrei* [28] was higher when exposed to AgNPs than when exposed to $AgNO_3$, whereas the growth and cocoon production of *Lumbricus rubellus* were more reduced by $AgNO_3$ than by AgNPs [29]. It should be noted that toxicity in these studies was related to total soil concentrations, not to available concentrations in the soil solution.

The higher toxicity of $AgNO_3$ may indicate that ionic Ag is the major cause of the toxicity of AgNPs [30]. This suggests that in the present study the dissolved fraction of AgNP-PVP was mainly present as Ag^+ ions, as its toxicity was similar to that of $AgNO_3$ when expressed on the basis of the concentration in the solution phase of our test medium. The LC50 for AgNP-Cit was a factor of 10 higher than that of $AgNO_3$, suggesting that only a fraction of the Ag measured in the solution phase of the test medium was present as Ag^+ ions. Because much more Ag from AgNP-Cit was found in solution compared with $AgNO_3$ or AgNP-PVP, this also suggests that part of the AgNP-Cit did pass the 0.45-μm filter and stayed in solution. The dissolution of AgNP-PVP was reported to be faster than that of AgNP-Cit [28], which again supports the idea that the fraction of Ag^+ ions was lower for AgNP-Cit than for $AgNO_3$ and AgNP-PVP and that the toxicity of AgNP-PVP and AgNP-NO_3 was mainly the result of released Ag^+ ions.

When expressed on the basis of concentrations in the test animals, AgNP-Cit again was least toxic, with highest LC50inter and highest lethal body concentration. The similarity of LC50inter for $AgNO_3$ and AgNP-PVP suggests that in both cases uptake of the same Ag form, probably ionic Ag, occurred. Because of the electrostatic stabilization of citrate, AgNP-Cit is more prone to agglomeration and might agglomerate especially in the presence of Ca^{2+} within hours [11]. Thus, once taken up AgNP-Cit could be aggregated in biological fluids with various ingredients inside the body of the organism, and its (internal) bioavailability might be limited in spite of being taken up by the organism. Kwak et al. [28] also mentioned decreased bioavailability of AgNP-Cit to *E. andrei* because of its agglomeration in biological fluids. The higher LC50 and higher LC50inter for AgNP-Cit suggest, on the one hand, that uptake of nanoparticulate Ag occurred but, on the other hand, that the low toxicity of internalized AgNP-Cit might the result of internal agglomeration. A recent study [31] confirmed this by imaging Ag speciation inside cells. The ratio of AgNPs to total Ag was much lower in the cells than in the extracellular medium because of reactions with H_2O_2 (intracellular reactive oxygen species) to form Ag ions. In cells, most of the Ag ions bind with thiol groups of proteins to form complexes which are known to be less toxic [32].

Both types of AgNPs produced an increasing toxicity pattern over time, which was similar to that of $AgNO_3$, with their LC50s decreasing and reaching equilibrium after approximately 10 d. These results emphasize that exposure duration of a (standard) toxicity test could be critical because toxicity changes over time until equilibrium is reached.

Toxicokinetics and toxicodynamics of different Ag forms to E. crypticus

The overall Ag K_w was lower for AgNP-Cit (3.62 L/kg dry body wt/d) than for the other 2 Ag forms, whereas the K_{e1} was lowest for AgNP-PVP (Table 1). The similarity in K_w values for $AgNO_3$ and AgNP-PVP supports the conclusion that exposure was mainly to ionic Ag in both cases. The lower overall K_w for AgNP-Cit suggests that its bioavailable fraction was much lower. However, it should be noted that, on the one hand, K_w values calculated for the lower AgNP-Cit exposure concentrations were somewhat higher (Supplemental Data, Table S6) but not as high as the values for $AgNO_3$ and AgNP-PVP. On the other hand, Ag concentrations measured in *E. crypticus* were quite similar for all 3 Ag forms at similar exposure concentrations (Supplemental Data, Tables S5–S7), but at the higher exposure concentrations of AgNP-Cit they did exceed the toxic level (LCinter) determined for the other 2 Ag forms. This seems to support the suggestion that at least some of the AgNP-Cit was taken up in the nano form.

Since the fit of the toxicokinetics model was poor for $AgNO_3$ and Ag-Cit, K_w and K_{e1} values were also calculated for each concentration level separately. Individual K_w values increased with increasing concentration up to a certain concentration level and then decreased with increasing concentration (Supplemental Data, Tables S5–S7). The same trend was also observed in studies with Ni (3.42–30.6 L/kg dry body wt/d [17]) and Cd (0.104–0.214 kg/kg dry body wt/d [32]). He and van Gestel [17] explained this trend from the limited number of metal ion transporters in the membrane of the organism, which could be occupied at higher concentrations. In addition, toxic effects at high exposure concentrations may reduce metal uptake rate. This might also be the case for Ag. Supplemental Data, Figure S1 supports these observations: internal total Ag concentrations increased with total Ag concentrations in the water fraction and approached equilibrium at a certain exposure concentration. Fitting the Langmuir equation enabled quantification of the affinity of the different Ag forms for uptake, which may resemble K_L, whereas the maximum amount accumulated in the enchytraeid (C_{max}) may provide some idea of the type of Ag accumulated (ionic or nano form) in the body. Unfortunately, K_L and C_{max} values of $AgNO_3$ and the AgNPs were not significantly different, so no firm conclusions can be drawn from these data.

The overall K_{e1} value for $AgNO_3$ and AgNP-Cit was higher than that for AgNP-PVP (Table 1); however, when looking at the individual values for the different test concentrations they all ranged between 0.1 d^{-1} and 0.5 d^{-1} (Supplemental Data, Tables S5–S7). Because elimination rates basically depend on organism characteristics, this suggests that the form in which Ag was present in the test organisms may have been the same for all Ag compounds. Although the survival-based elimination rates (K_{e2}) were significantly different for $AgNO_3$ and AgNP-Cit, they all had the same order of magnitude. From this, we may not conclude that the type of Ag accumulated was different.

The LC50inter values were calculated with Equation 6, which relates survival to internal body concentrations. Whereas LC50s changed dramatically over time, LC50inter values for the different Ag compounds were quite similar across all time points. A similar result was obtained for Ni by He and van Gestel [17]. The LC50inter value might be a better parameter than LC50 to represent the toxicity of the compounds because the effects of time on toxicity are taken into account. However, internal concentrations may not always be a good representative parameter because the effective concentration (toxicodynamic process) that leads to toxicity is not taken into account. Lethal body concentrations of all Ag forms, calculated using BCF values for all ($AgNO_3$) or the lower exposure (AgNPs) concentrations, were quite similar to the LC50inter value, which indicates that internal concentration and effective concentration are almost the same.

CONCLUSION

The present study is the first to determine the bioaccumulation and effects of AgNPs in *E. crypticus*. The toxicity of AgNP-PVP, expressed on the basis of Ag concentrations in the solution phase of our test media, was similar to that of $AgNO_3$, whereas AgNP-Cit was less toxic. This shows that toxicity is strongly dependent on coating material, which may be related to different adsorption to the sand matrix of the test medium. Whereas LC50 based on external concentrations in the test medium decreased with time, LC50inter (based on internal body concentrations of Ag) did not change significantly over time. Therefore, LC50inter can be more representative of toxicity. This emphasizes the necessity for the integration of toxicodynamics and toxicokinetics studies for AgNPs. Moreover, standard toxicity tests with duration shorter than 10 d may cause overestimation of LC50s because of nonequilibrium conditions. Future studies should focus on the long-term exposure of organisms to AgNPs to assess their potential toxicity under realistic environmental conditions and the effect of dissolution rate. Internal Ag concentrations will also provide insight into the bioaccumulation of AgNPs upon exposure to soil porewater, which represents the most likely route of exposure for many organisms in soil. The results of the present study may be helpful for the planning of future toxicity studies with environmentally relevant soil media.

SUPPLEMENTAL DATA

Tables S1–S7.
Figure S1. (207 KB DOCX).

Acknowledgment—The authors thank R. Verweij for technical support in the experimental work. E. Topuz was funded by the Scientific and Technological Research Council of Turkey (TUBITAK) 2211 Grant Program for her PhD studies and by the EU COST ES1205 Short Term Scientific Mission for the present study.

Data availability—All data are available in the Supplemental Data file.

REFERENCES

1. Project on Emerging Technologies. Consumer products inventory: An inventory of nanotechnology-based consumer products introduced on the market. [cited 2015 March 30]. Available from: http://www.nanotechproject.org/cpi/.
2. Cleveland D, Long SE, Pennington PL, Cooper E, Fulton MH, Scott GI, Brewer T, Davis J, Petersen EJ, Wood L. 2012. Pilot estuarine mesocosm study on the environmental fate of silver nanomaterials leached from consumer products. *Sci Total Environ* 421–422:267–272.
3. Hedberg J, Skoglund S, Karlsson ME, Wold S, Wallinder IO, Hedberg Y. 2014. Sequential studies of silver released from silver nanoparticles in aqueous media simulating sweat, laundry detergent solutions and surface water. *Environ Sci Technol* 48:7314–7322.

4. Lombi E, Donner E, Scheckel KG, Sekine R, Lorenz C, Von Goetz N, Nowack B. 2014. Silver speciation and release in commercial antimicrobial textiles as influenced by washing. *Chemosphere* 111:352–358.
5. Von Goetz N, Lorenz C, Windler L, Nowack B, Heuberger M, Hungerbühler K. 2012. Migration of Ag- and TiO_2-(nano) particles from textiles into artificial sweat under physical stress: Experiments and exposure modeling. *Environ Sci Technol* 47:9979–9987.
6. Nowack B, Ranville JF, Diamond S, Gallego-Urrea JA, Metcalfe C, Rose J, Horne N, Koelmans AA, Klaine SJ. 2012. Potential scenarios for nanomaterial release and subsequent alteration in the environment. *Environ Toxicol Chem* 31:50–59.
7. Navarro E, Piccapietra F, Wagner B, Marconi F, Kaegi R, Odzak N, Sigg L, Behra R. 2008. Toxicity of silver nanoparticles to *Chlamydomonas reinhardtii*. *Environ Sci Technol* 42:8959–8964.
8. Ribeiro F, Gallego-Urrea JA, Jurkschat K, Crossley A, Hassellöv M, Taylor C, Soares AMVM, Loureiro S. 2014. Silver nanoparticles and silver nitrate induce high toxicity to *Pseudokirchneriella subcapitata*, *Daphnia magna* and *Danio rerio*. *Sci Total Environ* 466–467:232–241.
9. Zhao CM, Wang WX. 2011. Comparison of acute and chronic toxicity of silver nanoparticles and silver nitrate to *Daphnia magna*. *Environ Toxicol Chem* 30:885–892.
10. Powers CM, Yen J, Linney EA, Seidler FJ, Slotkin TA. 2010. Silver exposure in developing zebrafish (*Danio rerio*): Persistent effects on larval behavior and survival. *Neurotoxicol Teratol* 32:391–397.
11. Topuz E, Sigg L, Talinli I. 2014. A systematic evaluation of agglomeration of Ag and TiO_2 nanoparticles under freshwater relevant conditions. *Environ Pollut* 193:37–44.
12. Kaegi R, Voegelin A, Ort C, Sinnet B, Thalmann B, Krismer J, Hagendorfer H, Elumelu M, Mueller E. 2013. Fate and transformation of silver nanoparticles in urban wastewater systems. *Water Res* 47:3866–3877.
13. Navarro DA, Kirby JK, McLaughlin MJ, Waddington L, Kookana RS. 2014. Remobilisation of silver and silver sulphide nanoparticles in soils. *Environ Pollut* 193:102–110.
14. Klitzke S, Metreveli G, Peters A, Schaumann GE, Lang F. 2015. The fate of silver nanoparticles in soil solution—Sorption of solutes and aggregation. *Sci Total Environ*, in press. DOI: 10.1016/j.scitotenv.2014.10.108
15. Behra R, Sigg L, Clift MJD, Herzog F, Minghetti M, Johnston B, Alke PF, Rothen-Rutishauser B. 2013. Bioavailability of silver nanoparticles and ions: From a chemical and biochemical perspective. *Journal of the Royal Society Interface* 10:1–17.
16. Tourinho PS, van Gestel CAM, Lofts S, Svendsen C, Soares AMVM, Loureiro S. 2012. Metal-based nanoparticles in soil: Fate, behavior, and effects on soil invertebrates. *Environ Toxicol Chem* 31:1679–1692.
17. He E, van Gestel CAM. 2013. Toxicokinetics and toxicodynamics of nickel in *Enchytraeus crypticus*. *Environ Toxicol Chem* 32:1835–1841.
18. Huynh KA, Chen KL. 2011. Aggregation kinetics of citrate and polyvinylpyrrolidone coated silver nanoparticles in monovalent and divalent electrolyte solutions. *Environ Sci Technol* 45:5564–5571.
19. Castro-Ferreira MP, Roelofs D, van Gestel CAM, Verweij RA, Soares AMVM, Amorim MJB. 2012. *Enchytraeus crypticus* as model species in soil ecotoxicology. *Chemosphere* 87:122–127.
20. Didden W, Rombke J. 2001. Enchytraeids as indicator organisms for chemical stress in terrestrial ecosystems. *Ecotoxicol Environ Saf* 50:25–43.
21. Cornelis G, Kirby JK, Beak D, Chittleborough D, McLaughlin MJ. 2010. A method for determination of retention of silver and cerium oxide manufactured nanoparticles in soils. *Environ Chem* 7:298–308.
22. Hamilton MA, Russo RC, Thurston RV. 1977. Trimmed Spearman-Karber method for estimating median lethal concentrations in toxicity bioassays. *Environ Sci Technol* 11:714–719.
23. Odzak N, Kistler D, Behra R, Sigg L. 2014. Dissolution of metal and metal oxide nanoparticles in aqueous media. *Environ Pollut* 191:132–138.
24. Gomes SIL, Soares AMVM, Scott-Fordsmand JJ, Amorim MJB. 2013. Mechanisms of response to silver nanoparticles on *Enchytraeus albidus* (Oligochaeta): Survival, reproduction and gene expression profile. *J Haz Mat* 254–255:336–344.
25. Schlich K, Klawonn T, Terytze K, Hund-Rinke K. 2013. Effects of silver nanoparticles and silver nitrate in the earthworm reproduction test. *Environ Toxicol Chem* 32:181–188.
26. Waalewijn-Kool PL, Klein K, Forniés RM, van Gestel CAM. 2014. Bioaccumulation and toxicity of silver nanoparticles and silver nitrate to the soil arthropod *Folsomia candida*. *Ecotoxicology* 23:1629–1637.
27. Heckmann LH, Hovgaard MB, Sutherland DS, Autrup H, Besenbacher F, Scott-Fordsmand JJ. 2010. Limit-test toxicity screening of selected inorganic nanoparticles to the earthworm *Eisenia fetida*. *Ecotoxicology* 20:226–233.
28. Kwak JI, Lee WM, Kim SW, An YJ. 2014. Interaction of citrate-coated silver nanoparticles with earthworm coelomic fluid and related cytotoxicity in *Eisenia andrei*. *J Appl Toxicol* 34:1145–1154.
29. Van Der Ploeg MJCY, Handy RD, Waalewijn-Kool PL, Van Den Berg JHC, Rivera ZEH, Bovenschen J, Molleman B, Baveco JM, Tromp P, Peters RJB, Koopmans GF, Rietjens IMCM, Van Den Brink NW. 2012. Effects of silver nanoparticles (Nm-300k) on *Lumbricus rubellus* earthworms and particle characterization in relevant test matrices including soil. *Environ Chem* 33:743–752.
30. Kittler S, Greulich C, Diendorf J, Köller M, Epple M. 2010. Toxicity of silver nanoparticles increases during storage because of slow dissolution under release of silver ions. *Chem Mater* 22:4548–4554.
31. Hsiao IL, Hsieh YK, Wang CF, Chen IC, Huang YJ. 2015. Trojan-horse mechanism in the cellular uptake of silver. *Environ Sci Technol* 49:3813–3821.
32. Lock K, Janssen CR. 2001. Zinc and cadmium body burdens in terrestrial oligochaetes: Use and significance in environmental risk assessment. *Environ Toxicol Chem* 20:2067–2072.